



## Abstract

The GOMOS (Global Ozone Monitoring by Occultation of Stars) instrument on board the Envisat satellite measures the vertical composition of the atmosphere using the stellar occultation technique. While the night-time data of GOMOS are proved to be of good quality, the daytime observations are more challenging due to poorer signal-to-noise ratio. In this paper we present an alternative technique, which uses GOMOS limb scattered radiances instead of the stellar signal, to retrieve stratospheric ozone profiles. Like for many other limb-viewing instruments, GOMOS observations contain stray light at high altitudes. We introduce a method for removing the stray light and demonstrate its feasibility by comparing the corrected radiances against those from the OSIRIS (Optical Spectrograph & Infra Red Imaging System) instrument. For the retrieval of ozone profiles, an onion peeling method is used. The first validation results suggest that the retrieval of stratospheric ozone is possible with a typical accuracy better than 10% at 22–50 km. GOMOS has measured about 350 000 daytime profiles since 2002. The new retrieval method presented here makes this large amount of data finally available for scientific use.

## 1 Introduction

During the last few decades, extensive research efforts have been made to measure the vertical composition of the Earth's atmosphere. Numerous satellite instruments have been deployed specifically to observe the middle atmosphere using different measurement techniques, geometries, and wavelengths regions.

Limb-viewing instruments can directly observe solar or stellar signal as it is occulted by the atmosphere, but limb scattered indirect sunlight, or radiance, can be used as well. Compared to the nadir looking instruments, the limb-viewing technique can not achieve as good global coverage, but it yields superior vertical resolution. A major advantage of the stellar occultation technique is the possibility of night-time observations

AMTD

3, 4355–4382, 2010

## Retrieval of GOMOS limb ozone

S. Tukiainen et al.

Title Page

Abstract

Introduction

Conclusions

References

Tables

Figures

◀

▶

◀

▶

Back

Close

Full Screen / Esc

Printer-friendly Version

Interactive Discussion



which is essential for, e.g., polar night studies. A detailed information of the past and present middle atmosphere instruments can be found elsewhere (Grant, 1989; Qu et al., 2006).

The key element of the middle atmosphere is ozone, but there are several other observable species such as NO<sub>x</sub> and HO<sub>x</sub> compounds, BrO, OCIO, aerosols and even metals. It is typically the wavelength band of the instrument that restricts which species are possible to detect. The obvious advantage of satellite measurements is that large quantities of global data can be gathered over long periods of time. Recent middle atmosphere studies have increasingly aimed to utilize, and sometimes combine, large satellite data sets in order to understand how ozone (or other species) are changing in time (Jones et al., 2009; Kyrölä et al., 2010). The goal of course is to distinguish between natural variations and anthropogenic forcings in the atmosphere. Furthermore, long and consistent satellite data sets are crucial for validation of climate models.

The GOMOS (Global Ozone Monitoring by Occultation of Stars) instrument on board the Envisat satellite uses stellar occultation method to probe the atmosphere between 10 and 120 km. Since 2002, GOMOS has performed altogether almost one million measurements. The ozone profiles obtained from the night-time occultations are considered to have typically better than 5% accuracy in the stratosphere (van Gijsel et al., 2010; Renard et al., 2008; Meijer et al., 2004). However, the majority of the daytime ozone profiles retrieved from occultations are currently of poor quality and not suitable for scientific use.

In addition to the star signal, GOMOS also records the limb scattered sunlight during the daytime in similar way than e.g. OSIRIS (Optical Spectrograph & Infra Red Imaging System) on the Odin satellite (Llewellyn et al., 2004) and SCIAMACHY (SCanning Imaging Absorption SpectroMeter for Atmospheric CHartography) on Envisat (Gottwald et al., 2006). The first experiment to retrieve ozone profiles from the GOMOS limb signal was done by Taha et al. (2008), obtaining promising results. In this paper we present a new method to retrieve ozone from the GOMOS bright limb (GBL) measurements and show some initial validation results.

**Retrieval of GOMOS limb ozone**

S. Tukiainen et al.

Title Page

Abstract

Introduction

Conclusions

References

Tables

Figures

◀

▶

◀

▶

Back

Close

Full Screen / Esc

Printer-friendly Version

Interactive Discussion



## 2 GOMOS radiance measurements

GOMOS CCDs record light from the limb using three spatial bands. The central band measures the sum of the star and the limb scattered signal, while the upper and the lower bands measure only the limb contribution. In the operational occultation retrieval, the upper/lower band radiance is removed from the central band measurement to get the pure star signal, which is then used for the retrievals. This procedure is performed for the day and twilight observations but not for night measurements when no limb contribution is present.

### 2.1 Saturation

The GOMOS radiance measurements suffer from CCD saturation below 30 km in the 400–500 nm band. The saturated pixels are flagged in the Level 1 data but the flags are not correctly implemented in the version 5.00 of the Level 1 data. The effect of the saturation is clearly seen when looking at normalized radiances (measured radiances divided by a radiance spectrum from high altitude). A normalized radiance is also called *radiance ratio*. Figure 1 shows normalized radiances between 350 and 550 nm for a single scan (orbit 9758, star 83) and for a few altitudes. The upper panel is plotted using the current Level 1 data, and while the signal notably begins to saturate at 26 km, the flags are claiming the data to be good up to 24 km.

New Level 1 processing version, coming out in the end of 2010, includes improved saturation flags. The lower panel of Fig. 1 reveals that almost all saturated pixels are now flagged correctly. It is important to have correct saturation flags for the successful retrieval. A common strategy in the retrieval is to take advantage of the whole UV-optical region between 280–700 nm and use dozens or even hundreds of wavelengths. This way the profiles can be retrieved for a wide altitude range. If the saturation flags are incorrect, and also saturated pixels are used in the retrieval, errors in the retrieved profiles will greatly increase. In this study we ignored the whole 400–500 nm region to be sure that no saturated pixels were used in the retrieval.

## Retrieval of GOMOS limb ozone

S. Tukiainen et al.

Title Page

Abstract

Introduction

Conclusions

References

Tables

Figures

◀

▶

◀

▶

Back

Close

Full Screen / Esc

Printer-friendly Version

Interactive Discussion



## 2.2 Stray light

In addition to the CCD saturation, the GOMOS limb scatter measurements suffer from severe stray light contamination. Stray light refers to unwanted extra scattering observed by the instrument. Stray light is usually coming from source other than the intended source. The relative amount of the stray light in GOMOS radiances increases with the altitude and above 100 km the signal is pure stray light.

We use the following method to remove the stray light contamination from the radiances. We first define mean relative stray light spectrum

$$S(\lambda) = \frac{1}{n} \sum_{j=1}^n (I(\lambda, j) \hat{I}(\lambda_{500}, j)^{-1}), \quad (1)$$

where  $I(\lambda, j)$  are measured radiances and  $\hat{I}(\lambda_{500}, j)$  are the radiances at 500 nm. The altitude index  $j$  goes through the measurements above 100 km and  $\lambda$  denotes wavelength.

Then we compute a third degree least squares polynomial fit for each wavelength using measurements above  $\hat{z}$ ,  $90 \text{ km} \leq \hat{z} \leq 100 \text{ km}$ , as the fitting range. Stray light is then extrapolated for low altitudes so that the low altitude values are constrained with the spectral shape in Eq. (1). After that we do another polynomial fit using the measurements above  $\hat{z}$  and the new point at low altitude to estimate the stray light for the all measurement altitudes. Figure 2 illustrates the stray light calculation for one (400 nm) wavelength.

A few things should be noted about the algorithm. Wavelengths are treated independently, which can in practice produce artificial noise on the results. Another issue is that the optimal value of  $\hat{z}$  and the order of the polynomial fits are unknown, and the choices can affect the results, too.

In reality, the amount of stray light may actually vary as a function of altitude leading to abnormal results from the extrapolation. Stray light is dependent on the albedo

Title Page

Abstract

Introduction

Conclusions

References

Tables

Figures

◀

▶

◀

▶

Back

Close

Full Screen / Esc

Printer-friendly Version

Interactive Discussion



below the satellite, and therefore strong albedo gradients during the measurement can disturb the usually quite constant stray light flux at high altitudes.

### 3 Radiance comparison

In this section we compare GOMOS radiances with OSIRIS radiances. OSIRIS is a combined UV-optical and infrared instrument dedicated to limb scatter measurements. The instrument is flying on board the Odin satellite, launched in 2001. The OSIRIS Level 1 data is the latest version, reprocessed in the end of 2009. The GOMOS Level is also the most recent available version 5.00 from 2006. OSIRIS radiances are relatively clean of stray light below  $\sim 70$  km and therefore OSIRIS is a good reference for the validation of GOMOS radiances and the stray light correction algorithm.

The criteria shown in Table 1 were used to find coincident measurements between GOMOS and OSIRIS. Using the data from the year 2004, a total of 13 matching observations were found when applying the coincidence criteria and excluding data with solar zenith angle larger than 86 degrees. These observations are from a narrow narrow latitude band, around  $60^\circ$  S, from January and February 2004.

#### 3.1 Spectral resolution and noise

The spectral resolution of GOMOS is  $\sim 3$  nm, i.e. relatively low compared to  $\sim 1$  nm of OSIRIS. This is because the slit of GOMOS is much larger than of OSIRIS. The wider slit allows the tracking of occultating stars but it lowers the spectral resolution. Therefore, we convoluted the OSIRIS spectra with the GOMOS slit function. The best estimate of the slit function is shown in Fig. 3.

In addition to the weak spectral resolution, the GOMOS radiances are also much noisier than those of OSIRIS. This makes it challenging to retrieve trace gases whose absorption fingerprint is small. For example,  $\text{NO}_2$  is routinely retrieved from

## Retrieval of GOMOS limb ozone

S. Tukiainen et al.

Title Page

Abstract

Introduction

Conclusions

References

Tables

Figures

◀

▶

◀

▶

Back

Close

Full Screen / Esc

Printer-friendly Version

Interactive Discussion



OSIRIS data using the strong NO<sub>2</sub> absorption features in the 430–450 nm region. Figure 4 shows radiance ratios in this region for GOMOS and OSIRIS at 32 km. The absorption lines are barely recognizable in the GOMOS ratio, while the OSIRIS ratio is far cleaner. At higher altitudes the noise in GOMOS obscures the absorption lines even further and below ~30 km the region starts to saturate as shown in Fig. 1.

### 3.2 Absolute radiance

First, we analyze differences in the GOMOS and OSIRIS absolute radiances. The radiances were interpolated in wavelength and in altitude using linear interpolation. Radiance as a function of altitude changes non-linearly in the UV wavelengths but the high vertical sampling resolution of both instruments (1–2 km) allows linear interpolation to be feasible.

Figure 5 shows an example of an individual OSIRIS (orbit 15702, scan 25) and GOMOS (orbit 9778, star 83) match. At 50 km, the amount of stray light in the GOMOS radiance is prominent, especially in wavelengths above 400 nm. After the stray light removal, the overall agreement is significantly better but the removal algorithm has introduced some additional noise to the radiance.

Figure 6 presents median differences between OSIRIS and stray light corrected GOMOS radiances for two different altitudes (50 and 30 km). There seems to be a positive bias in the GOMOS radiance below 350 nm. The bias is increasing towards lower altitudes, being up to around 20% at 50 km and 40–60% at 30 km.

### 3.3 Radiance ratio

Instead of using absolute radiances, a common practice to counteract uncertainties e.g. from calibration and polarization is to normalize radiance spectra by a high altitude measurement. It may be a full spectrum from one altitude, typically around 50 km, or the reference can come from various altitudes depending on the wavelength.

## Retrieval of GOMOS limb ozone

S. Tukiainen et al.

Title Page

Abstract

Introduction

Conclusions

References

Tables

Figures

◀

▶

◀

▶

Back

Close

Full Screen / Esc

Printer-friendly Version

Interactive Discussion



## Retrieval of GOMOS limb ozone

S. Tukiainen et al.

Title Page

Abstract

Introduction

Conclusions

References

Tables

Figures

◀

▶

◀

▶

Back

Close

Full Screen / Esc

Printer-friendly Version

Interactive Discussion



The same match as in Fig. 5 is shown in Fig. 7 but the radiances are now normalized with the 47 km spectra. The difference in the UV band is apparent and the stray light corrected ratio is noisier than the original GOMOS radiance ratio. Otherwise the agreement between the OSIRIS ratio and the stray light corrected GOMOS ratio is good.

The median of the differences of the 13 matches is shown in Fig. 8 for 55 and 30 km. At 30 km the GOMOS ratio is biased up to +20% below 320 nm and there is an opposed bias at 55 km. At 55 km the red end of the spectrum is quite noisy due to the stray light correction. The bias in the wavelengths 320–680 nm is 5–10 % for both investigated altitudes.

## 4 Inversion method

A slightly revised version of the inversion method described in detail in Tukiainen et al. (2008) is used for the retrieval. The fundamental idea is the same. For every measurement layer  $j$ , a least squares fit weighted by error is done between the model and measurement:

$$\frac{I(j, \lambda)}{I_{\text{ref}}(\lambda)} = \frac{\hat{I}_{\text{ss}}(j, \lambda, \rho)}{\hat{I}_{\text{ref}}(\lambda)} R(j, \lambda) + \epsilon, \quad (2)$$

where  $I(j, \lambda)$  is the observed radiance and  $I_{\text{ref}}(\lambda)$  is a reference measurement at  $\sim 50$  km. On the right hand side,  $\hat{I}_{\text{ss}}(j, \lambda, \rho)$  is the modeled single scattering radiance, adjusted dynamically during the fitting operations, and  $\hat{I}_{\text{ref}}(\lambda)$  is the modeled reference radiance. The second term on the right:

$$R(j, \lambda) = \frac{\hat{I}_{\text{tot}}(j, \lambda)}{\hat{I}_{\text{ss}}(j, \lambda)} \quad (3)$$

is the ratio of modeled total to single scattering radiance. This term comes from a look-up-table and is kept fixed during iterations. The iterative fitting of gas densities  $\rho$  in

**Retrieval of GOMOS  
limb ozone**

S. Tukiainen et al.

[Title Page](#)[Abstract](#)[Introduction](#)[Conclusions](#)[References](#)[Tables](#)[Figures](#)[◀](#)[▶](#)[◀](#)[▶](#)[Back](#)[Close](#)[Full Screen / Esc](#)[Printer-friendly Version](#)[Interactive Discussion](#)

Eq. (2) is done using the Levenberg-Marquardt method (Levenberg, 1944; Marquardt, 1963). The error term  $\epsilon$  in Eq. (2) is used as a weight in the fitting.

The atmosphere between around 60 and 20 km is “peeled” this way from top to down to get the vertical profiles of retrieved species. With this approach, it is possible to retrieve several species simultaneously. Typically  $O_3$ , aerosols and neutral air are inverted together using tens (or hundreds) of wavelengths in the 280–680 nm band, while  $NO_2$  is taken from a climatology and kept fixed. However, as shown in Tukiainen et al. (2008), it is better to retrieve minor absorbers such as  $NO_2$  in a separate peeling loop using much smaller wavelength windows. It should be noted that, as mentioned earlier,  $NO_2$  is not currently retrieved from the GOMOS bright limb measurements due to weak spectral fingerprint in the 430–450 nm band.

### Radiative transfer model

It is straightforward and computationally very effective to calculate single scattering radiances in limb-viewing geometry. But in the visible wavelengths, a significant part of the photons have been scattered multiple times before observed by the instrument. This makes the modeling challenging, and usually approximations are used to simplify the radiative transfer calculations.

Several models have been developed to calculate the multiple scattering radiance of the radiative transfer problem in the UV visible wavelengths. The more modern ones include eg. SASKTRAN (Bourassa et al., 2008), McSCIA (Spada et al., 2006), Sciatran (Roazanov et al., 2005), MCC++ (Postlylyakov, 2004), LIMBTRAN (Griffioen and Oikarinen, 2000) and Siro (Oikarinen et al., 1999).

We use a revised version of the Monte Carlo (MC) model Siro. Siro is a backward MC model – the photons are simulated from the detector towards the atmosphere. The latest Siro version is written in Fortran90 and parallelized using OpenMP framework. Options for polarization and refraction are available, but were not used in this study.

The execution time of Siro depends mainly on the tangent point altitude and wavelength. More multiple scattering means slower execution. Smaller contributions come

from the solar angles, atmospheric composition and albedo. The running time, and precision of the solution, is naturally proportional to the number of simulated photons. With a modern CPU (Xeon E5420) using only single core, a  $10^5$  photon simulation for one wavelength takes a few seconds in the UV region. In the visible band, a similar simulation takes typically around 30 s.

It is computationally too expensive to use Siro directly in the operational retrieval. Instead in Eq. (2) we use a fast analytical single scattering model and perform multiple scattering correction using a Siro calculated look-up table. The Siro look-up table is built with the parameters shown in Table 2. To get approximately 1% accuracy, radiances were simulated with  $10^5$  photons.

## 5 Ozone profile validation

As there is some discrepancy in the GOMOS and OSIRIS radiances below  $\sim 350$  nm, differences in retrieved ozone profiles should be expected. Above around 45 km, these wavelengths are required for successful ozone retrieval. But at lower altitudes, the information mainly comes from the Chappuis band around 600 nm, and the UV band can be suppressed from the inversion to cope with the issue.

Figure 9 shows a comparison of the 13 GOMOS bright limb and OSIRIS ozone profile retrieved using the radiances shown in Figs. 6 and 8. The medians of the profiles are shown in the left panel. The GOMOS profiles were retrieved with the UV band (red dashed line) and without the UV band below 45 km (red solid line). The right panel shows the medians of the individual relative differences. In both cases there is a negative bias below 50 km compared to OSIRIS but flagging the UV wavelengths clearly improves the agreement.

To better test the statistical accuracy of the retrieved profiles, we compare the GOMOS bright limb profiles with the GOMOS night-time occultation profiles. Due to issues in the 400–500 nm band (saturation) and in the UV band below 45 km, we flagged these wavelengths from the retrieval. Figure 10 shows the result of the comparison in

## Retrieval of GOMOS limb ozone

S. Tukiainen et al.

Title Page

Abstract

Introduction

Conclusions

References

Tables

Figures

◀

▶

◀

▶

Back

Close

Full Screen / Esc

Printer-friendly Version

Interactive Discussion



the equator between 30° S and 30° N. The 79 profiles are from 2003 with no more than 1° difference in latitude, 2° in longitude and 15 h in time. The median of the individual relative differences is less than 10% between 22 and 50 km. Above 45 km the diurnal variation of ozone starts to take effect, and the GBL values (day) are smaller than the night occultation values, as expected. Below 22 km the standard deviation of the GBL profiles increase significantly. It is difficult to follow occultating stars at low tangent altitudes, and especially when clouds enter the line of sight.

## 6 Discussion

There are serious defects in the GOMOS Level 1 bright limb data that complicate trace gas retrievals. The stray light contamination is a severe problem at high altitudes. In the wavelengths >400 nm, stray light accounts for as much as 10–50% of the measured signal already at the 50 km altitude (see Fig. 5). Thus, it is absolutely necessary to correct for the stray light. The radiance comparisons against OSIRIS suggest that the algorithm presented in Sect. 2.2 is feasible.

In addition to the stray light, the signal saturates below around 30 km in the 400–500 nm region making a large part of the spectrum useless. Current saturation flags are not trustworthy, but the situation is greatly improved with the upcoming version of the Level 1 data.

The spectral resolution of GOMOS (bright limb signal) is poor, about 3 nm compared to the ~1 nm resolution of OSIRIS. The spectra of GOMOS are also noisier than those of OSIRIS. Both the weak spectral resolution and the noise make NO<sub>2</sub> retrieval difficult and so far it has not been successful.

Furthermore, there seems to be a systematic difference between the GOMOS and OSIRIS spectra in the wavelengths below 320 nm. This cannot be explained by the stray light because the discrepancy increases at lower altitudes where the relative amount of stray light decreases. The difference is apparent in both absolute and normalized radiance (see Figs. 6 and 8). Unfortunately, close matches between

## Retrieval of GOMOS limb ozone

S. Tukiainen et al.

Title Page

Abstract

Introduction

Conclusions

References

Tables

Figures

◀

▶

◀

▶

Back

Close

Full Screen / Esc

Printer-friendly Version

Interactive Discussion



OSIRIS and GOMOS measurement times, tangent point locations, and solar angles are rare and only 13 cases were investigated in this paper.

The disagreement in the UV band leads to a difference in the retrieved ozone profiles between GOMOS bright limb and OSIRIS. It is possible to cope with the problem by suppressing the UV band in the retrieval below  $\sim 45$  km. After flagging the UV band (and the saturation band) the agreement with GOMOS night-time occultations was better than 10% between 22 and 50 km in the equator. The good validation result against the GOMOS night-time occultations, after flagging the UV band, suggest that the UV band is biased indeed in GOMOS and not in OSIRIS.

Despite the weaknesses in the Level 1 data, the proposed stray light removal algorithm and the inversion method offer a promising way to utilize the whole GOMOS bright limb data set. The processing of the GBL data would roughly double the amount of useful GOMOS ozone profiles between at least 22 and 50 km. The distribution of GOMOS night-time and daytime measurements in 2004 is shown in Fig. 11.

Finally, it should be noted that the validation for profiles shown in this paper are preliminary and should be repeated using other reference instruments for all latitudes. Additionally, the robustness and performance of the stray light correction could be analyzed more carefully in a separate study.

*Acknowledgements.* This work was funded by the European Space Agency through the project *Trace Gas Retrieval from GOMOS Bright Limb Measurements* (AO/1-5301/06/I-OL). The authors wish to thank Marko Laine, Seppo Hassinen, Benjamin Herman, Anne van Gijssel, and Ankie Piters for their valuable help.

**Retrieval of GOMOS limb ozone**

S. Tukiainen et al.

Title Page

Abstract Introduction

Conclusions References

Tables Figures

◀ ▶

◀ ▶

Back Close

Full Screen / Esc

Printer-friendly Version

Interactive Discussion



Discussion Paper | Discussion Paper | Discussion Paper | Discussion Paper | Discussion Paper

## References

- Bourassa, A. E., Degenstein, D. A., and Llewellyn, E. J.: SASKTRAN: a spherical geometry radiative transfer code for efficient estimation of limb scattered sunlight, *J. Quant. Spectrosc. Ra.*, 109, 52–73, doi:10.1016/j.jqsrt.2007.07.007, 2008. 4363
- 5 Gottwald, M., Bovensmann, H., Lichtenberg, G., Noel, S., von Bargaen, A., Slijkhuis, S., Piters, A., Hoogeveen, R., von Savigny, C., Buchwitz, M. A. K., Richter, A., Rozanov, A., Holzer-Popp, T., Bramstedt, K., Lambert, J.-C., Skupin, J., Wittrock, F., Schrijver, H., and Burrows, J.: SCIAMACHY, Monitoring the Changing Earth's Atmosphere, DLR, 2006. 4357
- 10 Grant, W. B.: Ozone Measuring Instruments for the Stratosphere, Optical Society of America, Washington, 1989. 4357
- Griffioen, E. and Oikarinen, L.: LIMBTRAN: A pseudo three-dimensional radiative transfer model for the limb-viewing imager OSIRIS on the ODIN satellite, *J. Geophys. Res.*, 105, 29717–29730, doi:10.1029/2000JD900566, 2000. 4363
- 15 Jones, A., Urban, J., Murtagh, D. P., Eriksson, P., Brohede, S., Haley, C., Degenstein, D., Bourassa, A., von Savigny, C., Sonkaew, T., Rozanov, A., Bovensmann, H., and Burrows, J.: Evolution of stratospheric ozone and water vapour time series studied with satellite measurements, *Atmos. Chem. Phys.*, 9, 6055–6075, doi:10.5194/acp-9-6055-2009, 2009. 4357
- Kyrölä, E., Tamminen, J., Sofieva, V., Bertaux, J. L., Hauchecorne, A., Dalaudier, F., Fussen, D., Vanhellefont, F., Fanton d'Andon, O., Barrot, G., Guirlet, M., Fehr, T., and Saavedra de Miguel, L.: GOMOS O<sub>3</sub>, NO<sub>2</sub>, and NO<sub>3</sub> observations in 2002–2008, *Atmos. Chem. Phys.*, 10, 7723–7738, doi:10.5194/acp-10-7723-2010, 2010. 4357
- 20 Levenberg, K.: A method for the solution of certain problems in least squares, *Q. Appl. Math.*, 2, 164–168, 1944. 4363
- Llewellyn, E., Lloyd, N. D., Degenstein, D. A., Gattinger, R. L., Petelina, S. V., Bourassa, A. E., Wiensz, J. T., Ivanov, E. V., McDade, I. C., Solheim, B. H., McConnell, J. C., Haley, C. S., von Savigny, C., Sioris, C. E., McLinden, C. A., Griffioen, E., Kaminski, J., Evans, W. F. J., Puckrin, E., Strong, K., Wehrle, V., Hum, R. H., Kendall, D. J. W., Matsushita, J., Murtagh, D. P., Brohede, S., Stegman, J., Witt, G., Barnes, G., Payne, W. F., Piche, L., Smith, K., Warshaw, G., Deslauniers, D. L., Marchand, P., Richardson, E. H., King, R. A., Wevers, I., McCreath, W., Kyrola, E., Oikarinen, L., Leppelmeier, G. W., Auvinen, H., Megie, G., Hauchecorne, A., Lefevre, F., de La Noe, J., Ricaud, P., Frisk, U., Sjoberg, F., von Scheele, F., and Nordh, L.: The OSIRIS instrument on the Odin spacecraft, *Can. J. Phys.*, 82, 411–422,
- 25
- 30

AMTD

3, 4355–4382, 2010

## Retrieval of GOMOS limb ozone

S. Tukiainen et al.

Title Page

Abstract

Introduction

Conclusions

References

Tables

Figures

◀

▶

◀

▶

Back

Close

Full Screen / Esc

Printer-friendly Version

Interactive Discussion



## Retrieval of GOMOS limb ozone

S. Tukiainen et al.

Title Page

Abstract

Introduction

Conclusions

References

Tables

Figures

◀

▶

◀

▶

Back

Close

Full Screen / Esc

Printer-friendly Version

Interactive Discussion



doi:10.1139/p04-005, 2004. 4357

Marquardt, D.: An algorithm for least-squares estimation of nonlinear parameters, *J. Soc. Indust. Appl. Math.*, 11, 431–44, 1963. 4363

Meijer, Y. J., Swart, D. P. J., Allaart, M., Andersen, S. B., Bodeker, G., Boyd, I., Braathen, G., Calisesi, Y., Dorokhov, V., Claude, H., von der Gathen, P., Gil, M., Godin-Beekmann, S., Goutail, F., Hansen, G., Karpetchko, A., Keckhut, P., Kelder, H. M., Koelemeijer, R. K., Kois, B., Koopman, R. M., Lambert, J.-C., Leblanc, T., McDermid, I. S., Pal, S., Kopp, G., Schets, H., Stubi, R., Suortti, T., Visconti, G., and Yela, M.: Pole-to-pole validation of ENVISAT/GOMOS ozone profiles using data from ground-based and balloon-sonde measurements, *J. Geophys. Res.*, 109, D23305, doi:10.1029/2004JD004834, 2004. 4357

Oikarinen, L., Sihvola, E., and Kyrölä, E.: Multiple scattering radiance in limb-viewing geometry, *J. Geophys. Res.*, 104, 31261–31274, doi:10.1029/1999JD900969, 1999. 4363

Postylyakov, O. V.: Radiative transfer model MCC++ with evaluation of weighting functions in spherical atmosphere for use in retrieval algorithms, *Adv. Space Res.*, 34, 721–726, doi:10.1016/j.asr.2003.07.070, 2004. 4363

Qu, J., Gao, W., Kafatos, M., Murphy, R., and Salomonson, V.: *Earth Science Satellite Remote Sensing Vol. 1: Science and Instruments*, Springer, 2006. 4357

Renard, J., Berthet, G., Brogniez, C., Catoire, V., Fussen, D., Goutail, F., Oelhaf, H., Pomereau, J., Roscoe, H. K., Wetzell, G., Chartier, M., Robert, C., Balois, J., Verwaerde, C., Auriol, F., François, P., Gaubicher, B., and Wursteisen, P.: Validation of GOMOS-Envisat vertical profiles of O<sub>3</sub>, NO<sub>2</sub>, NO<sub>3</sub>, and aerosol extinction using balloon-borne instruments and analysis of the retrievals, *J. Geophys. Res.-Space*, 113, A02302, doi:10.1029/2007JA012345, 2008. 4357

Rozanov, A., Rozanov, V., Buchwitz, M., Kokhanovsky, A., and Burrows, J. P.: SCIATRAN 2.0 A new radiative transfer model for geophysical applications in the 175–2400 nm spectral region, *Adv. Space Res.*, 36, 1015–1019, doi:10.1016/j.asr.2005.03.012, 2005. 4363

Spada, F., Krol, M. C., and Stammes, P.: McSCIA: application of the Equivalence Theorem in a Monte Carlo radiative transfer model for spherical shell atmospheres, *Atmos. Chem. Phys.*, 6, 4823–4842, doi:10.5194/acp-6-4823-2006, 2006. 4363

Taha, G., Jaross, G., Fussen, D., Vanhellefont, F., Kyrölä, E., and McPeters, R. D.: Ozone profile retrieval from GOMOS limb scattering measurements, *J. Geophys. Res.*, 113, D23307, doi:10.1029/2007JD009409, 2008. 4357

Tukiainen, S., Hassinen, S., Seppälä, A., Auvinen, H., Kyrölä, E., Tamminen, J., Haley, C. S., Lloyd, N., and Verronen, P. T.: Description and validation of a limb scatter retrieval method for Odin/OSIRIS, *J. Geophys. Res.*, 113, D04308, doi:10.1029/2007JD008591, 2008. 4362, 4363

- 5 van Gijsel, J. A. E., Swart, D. P. J., Baray, J.-L., Bencherif, H., Claude, H., Fehr, T., Godin-Beekmann, S., Hansen, G. H., Keckhut, P., Leblanc, T., McDermid, I. S., Meijer, Y. J., Nakane, H., Quel, E. J., Stebel, K., Steinbrecht, W., Strawbridge, K. B., Tatarov, B. I., and Wolfram, E. A.: GOMOS ozone profile validation using ground-based and balloon sonde measurements, *Atmos. Chem. Phys. Discuss.*, 10, 8515–8551, doi:10.5194/acpd-10-8515-2010, 2010. 4357

# AMTD

3, 4355–4382, 2010

## Retrieval of GOMOS limb ozone

S. Tukiainen et al.

Title Page

Abstract

Introduction

Conclusions

References

Tables

Figures

◀

▶

◀

▶

Back

Close

Full Screen / Esc

Printer-friendly Version

Interactive Discussion



**Retrieval of GOMOS  
limb ozone**

S. Tukiainen et al.

Title Page

Abstract

Introduction

Conclusions

References

Tables

Figures

I◀

▶I

◀

▶

Back

Close

Full Screen / Esc

Printer-friendly Version

Interactive Discussion

**Table 1.** Coincidence criteria for the GOMOS and OSIRIS radiance matches.

Latitude	3°
Longitude	6°
Time	24 h
Sun zenith angle	2°
Scattering angle	2°



## Retrieval of GOMOS limb ozone

S. Tukiainen et al.

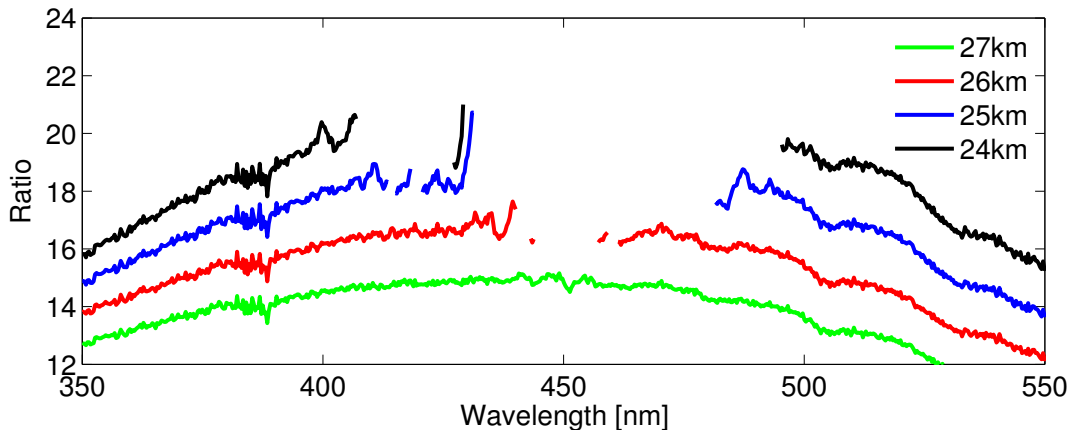
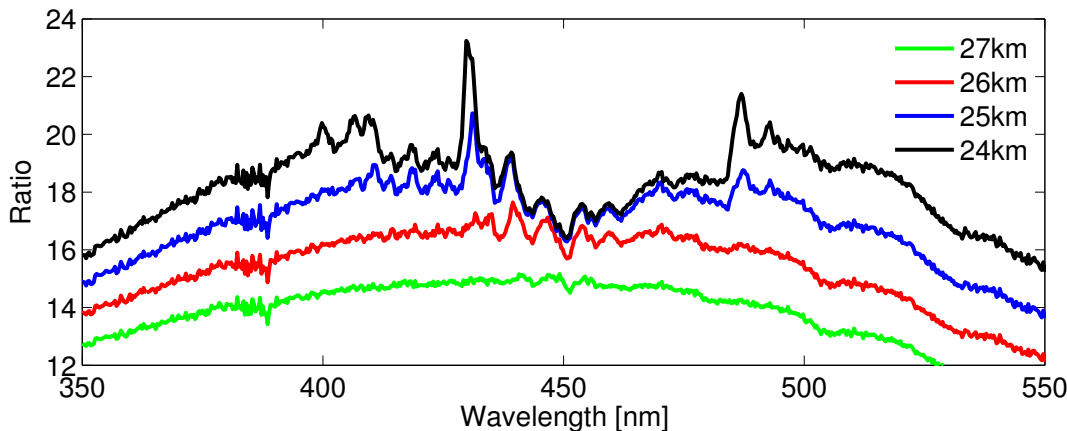


**Fig. 1.** Saturation in the normalized GOMOS radiances for a few altitudes. Upper panel: current Level 1 version, where obviously saturated pixels are not flagged. Lower panel: forthcoming Level 1 version including improved saturation flags (data achieved via private communications with Gilbert Barrot, ACRI-ST).

Title Page	
Abstract	Introduction
Conclusions	References
Tables	Figures
◀	▶
◀	▶
Back	Close
Full Screen / Esc	
Printer-friendly Version	
Interactive Discussion	



## Retrieval of GOMOS limb ozone

S. Tukiainen et al.

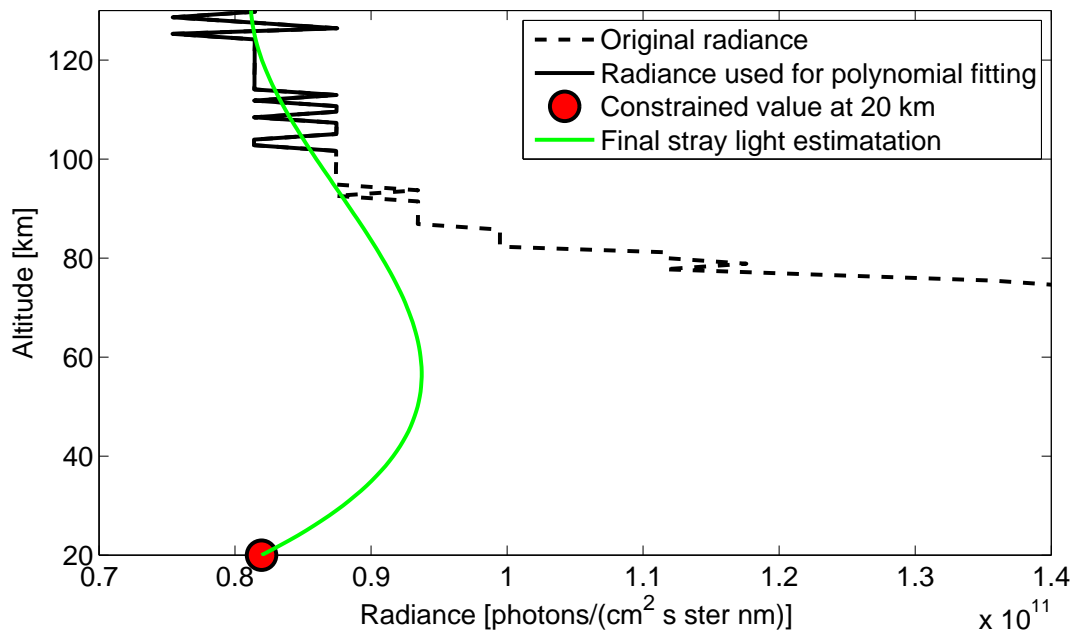


**Fig. 2.** Stray light estimation for 400 nm. The spectral shape of the stray light is used to calculate the 20 km point (red circle), which is then used together with the >100 km radiance values to calculate the stray light for all altitudes.

Title Page

Abstract

Introduction

Conclusions

References

Tables

Figures

◀

▶

◀

▶

Back

Close

Full Screen / Esc

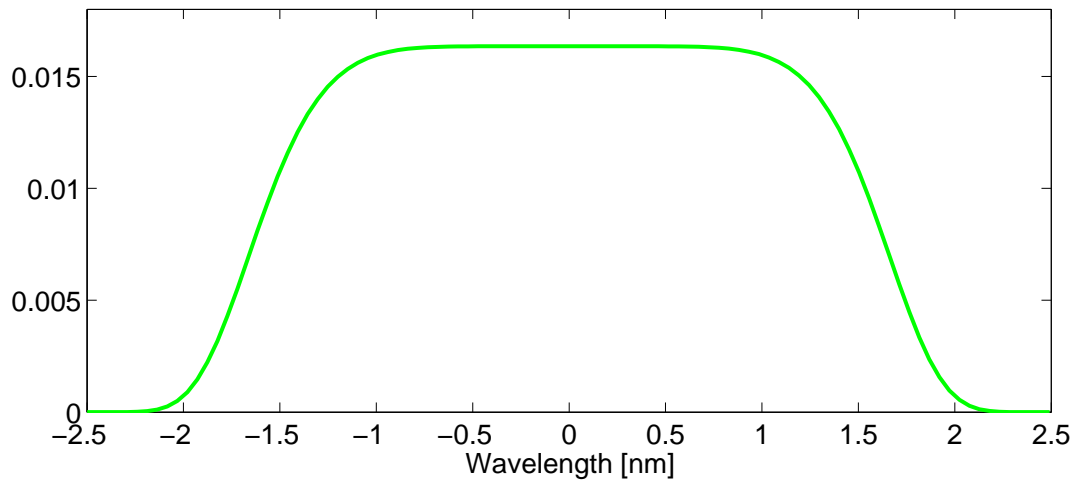
Printer-friendly Version

Interactive Discussion



**Retrieval of GOMOS limb ozone**

S. Tukiainen et al.

**Fig. 3.** GOMOS slit function.[Title Page](#)[Abstract](#)[Introduction](#)[Conclusions](#)[References](#)[Tables](#)[Figures](#)[◀](#)[▶](#)[◀](#)[▶](#)[Back](#)[Close](#)[Full Screen / Esc](#)[Printer-friendly Version](#)[Interactive Discussion](#)

**Retrieval of GOMOS limb ozone**

S. Tukiainen et al.

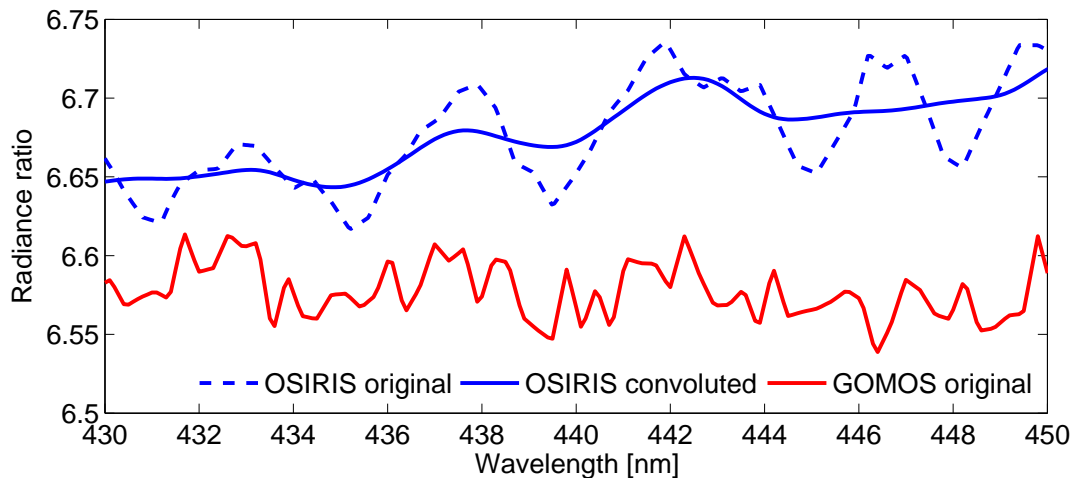


**Fig. 4.** Comparison of GOMOS and OSIRIS spectral resolution in the  $\text{NO}_2$  retrieval region. Shown are 32 km radiances normalized with the 47 km spectra. The GOMOS ratio is before stray light correction and scaled to fit in the figure.

[Title Page](#)[Abstract](#)[Introduction](#)[Conclusions](#)[References](#)[Tables](#)[Figures](#)[◀](#)[▶](#)[◀](#)[▶](#)[Back](#)[Close](#)[Full Screen / Esc](#)[Printer-friendly Version](#)[Interactive Discussion](#)

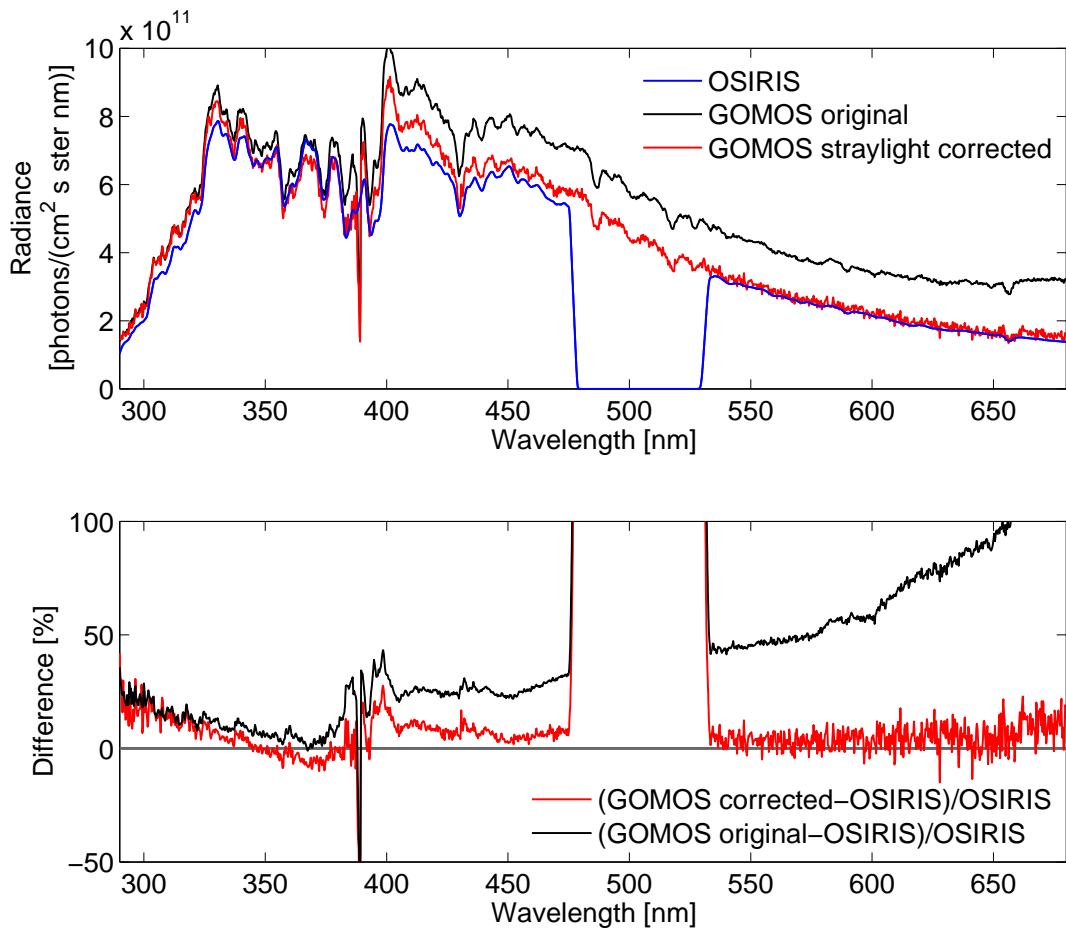


**Fig. 5.** Example of the absolute radiances from from GOMOS (orbit 9778, star 83) and OSIRIS (orbit 15702, scan 25). Upper panel: radiances at 50 km. Lower panel: relative differences.

**Retrieval of GOMOS limb ozone**

S. Tukiainen et al.

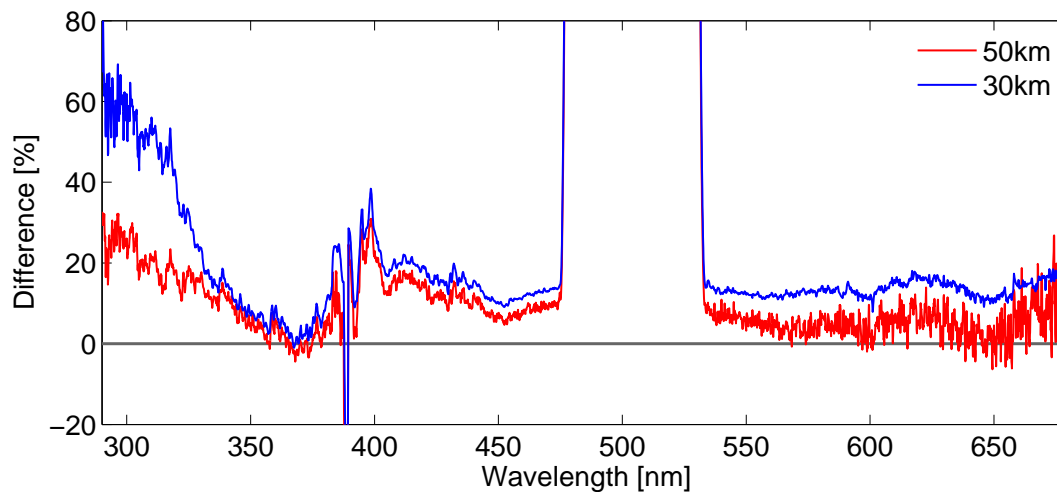


**Fig. 6.** Median relative difference of the 13 OSIRIS and stray light corrected GOMOS absolute radiances at 30 km (blue) and 50 km (red).

[Title Page](#)[Abstract](#)[Introduction](#)[Conclusions](#)[References](#)[Tables](#)[Figures](#)[◀](#)[▶](#)[◀](#)[▶](#)[Back](#)[Close](#)[Full Screen / Esc](#)[Printer-friendly Version](#)[Interactive Discussion](#)

## Retrieval of GOMOS limb ozone

S. Tukiainen et al.

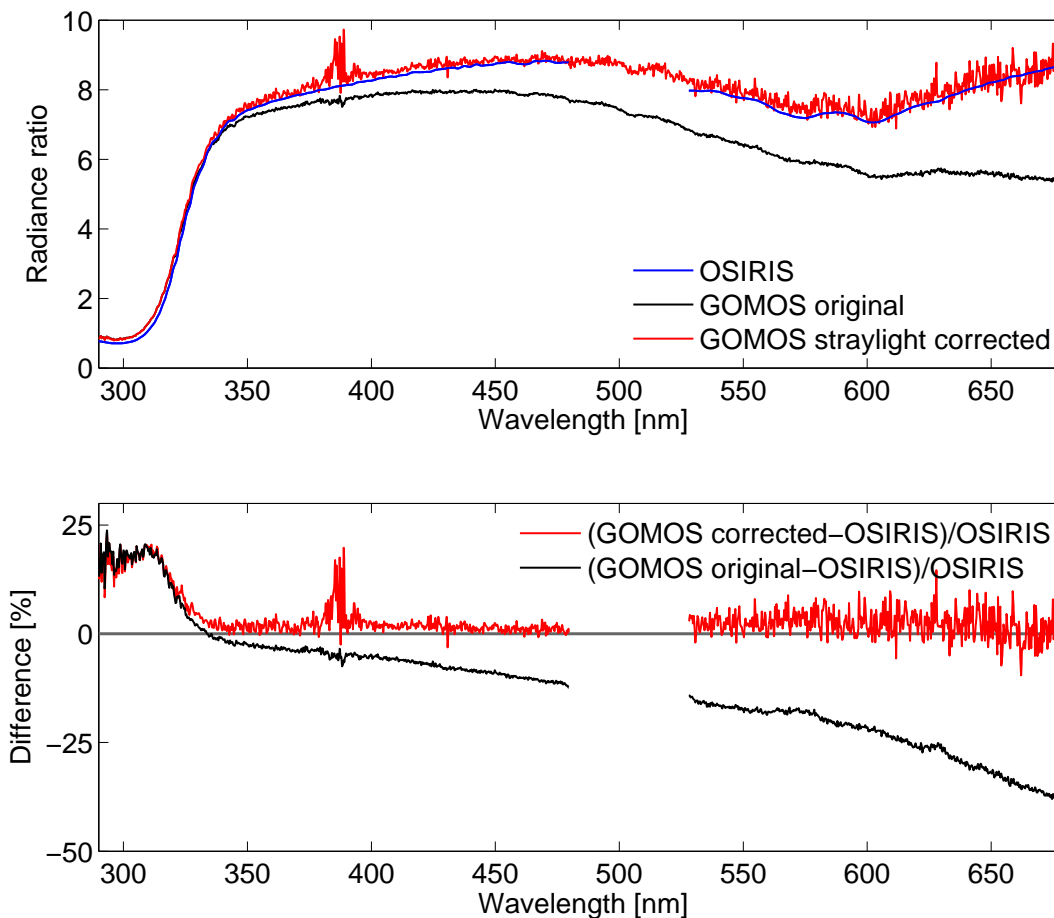


**Fig. 7.** Example of radiance ratio from from GOMOS (orbit 9778, star 83) and OSIRIS (orbit 15702, scan 25). Upper panel: ratios of 30 and 47 km. Lower panel: relative differences.

Title Page

Abstract Introduction

Conclusions References

Tables Figures

◀ ▶

◀ ▶

Back Close

Full Screen / Esc

Printer-friendly Version

Interactive Discussion



**Retrieval of GOMOS limb ozone**

S. Tukiainen et al.

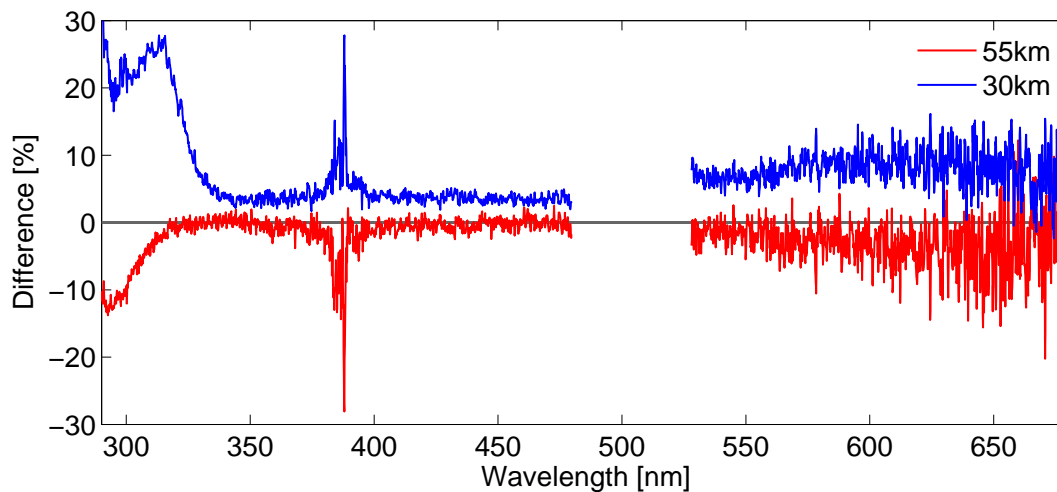


**Fig. 8.** Median relative difference of the 13 OSIRIS and stray light corrected GOMOS radiance ratios at 30 km (blue) and 55 km (red). Radiances were normalized with the 47 km spectrum.

[Title Page](#)[Abstract](#)[Introduction](#)[Conclusions](#)[References](#)[Tables](#)[Figures](#)[◀](#)[▶](#)[◀](#)[▶](#)[Back](#)[Close](#)[Full Screen / Esc](#)[Printer-friendly Version](#)[Interactive Discussion](#)

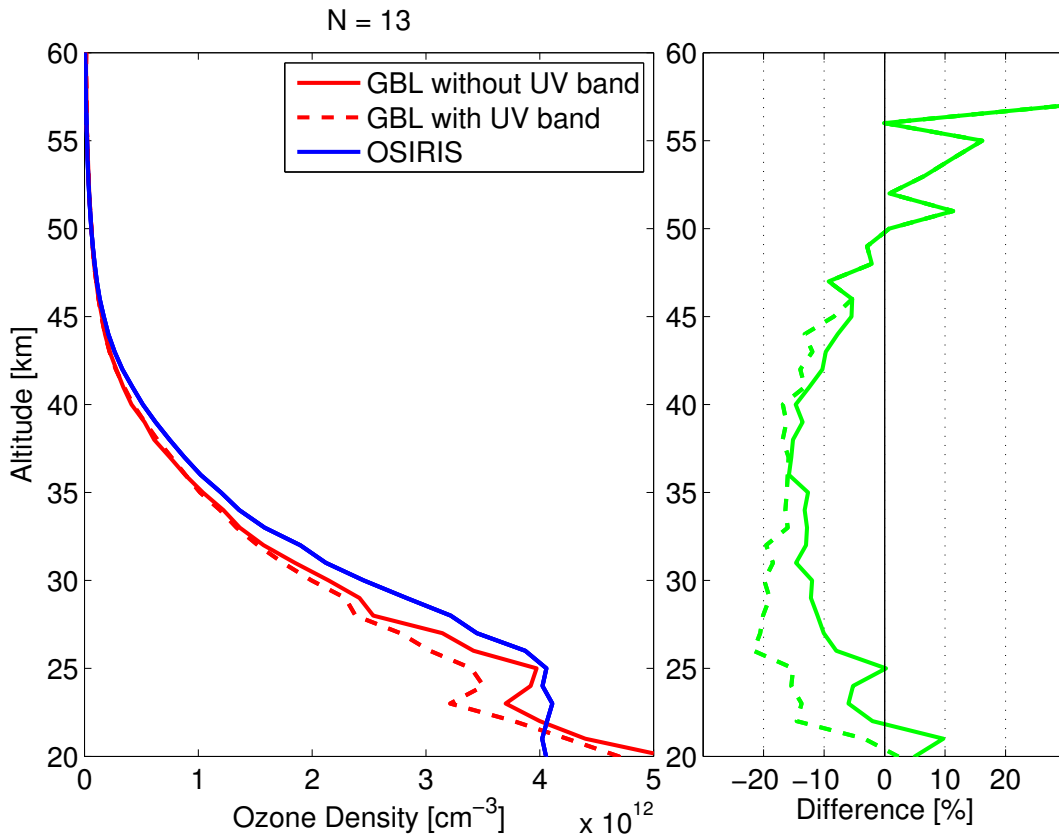


**Fig. 9.** Retrieved ozone profiles from the 13 GOMOS and OSIRIS radiances of Figs. 6 and 8. The GOMOS profiles were retrieved with the UV band (red dashed profile) and without using the UV band below 45 km (red solid profile). Right panel: medians of individual relative differences compared to the OSIRIS profiles.

**Retrieval of GOMOS limb ozone**

S. Tukiainen et al.

Title Page

Abstract Introduction

Conclusions References

Tables Figures

◀ ▶

◀ ▶

Back Close

Full Screen / Esc

Printer-friendly Version

Interactive Discussion



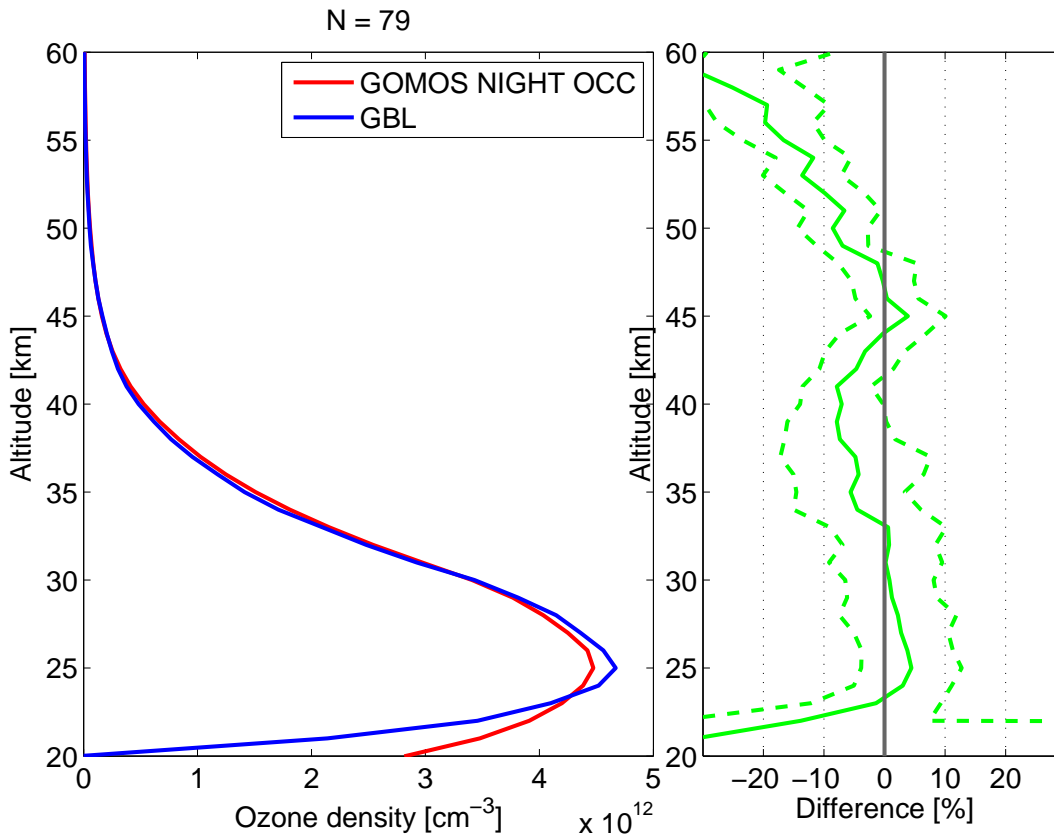


**Fig. 10.** Comparison of the 79 GOMOS bright limb profiles and GOMOS night occultations at equator. Left panel: medians of the distributions. Right panel: median of the individual differences (solid) and the 50% percentiles (dashed).

**Retrieval of GOMOS limb ozone**

S. Tukiainen et al.

Title Page

Abstract Introduction

Conclusions References

Tables Figures

◀ ▶

◀ ▶

Back Close

Full Screen / Esc

Printer-friendly Version

Interactive Discussion



**Retrieval of GOMOS limb ozone**

S. Tukiainen et al.

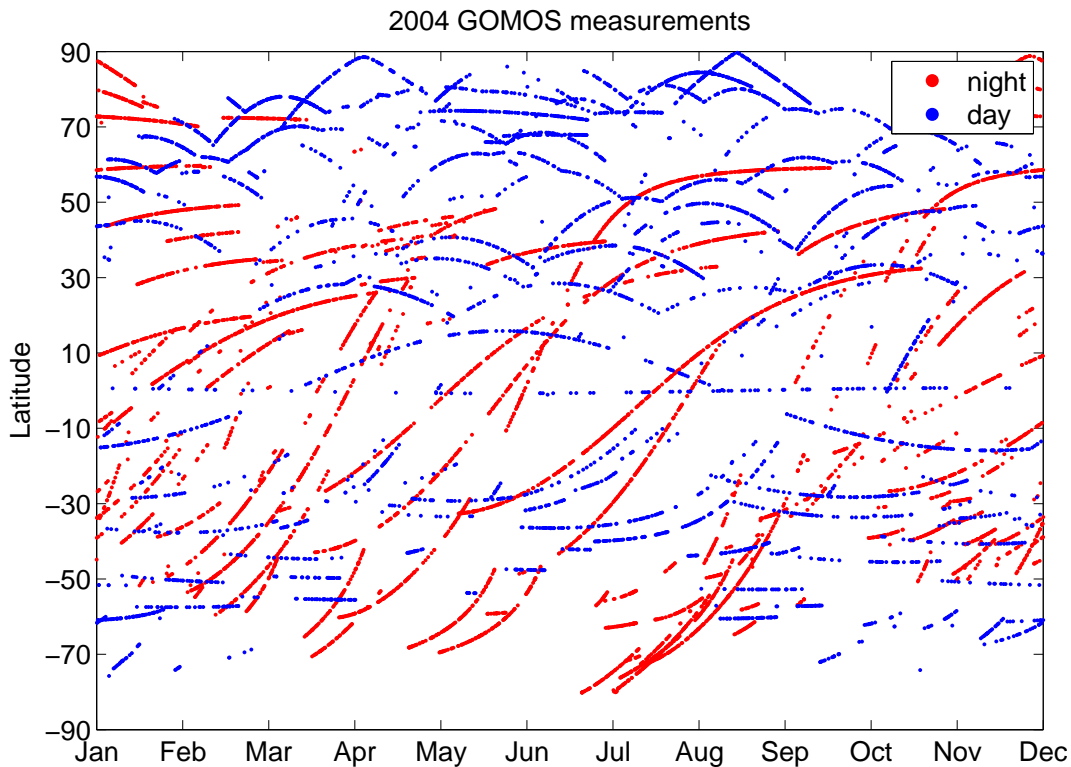


**Fig. 11.** Distribution of the night and daytime measurements from GOMOS during 2004.

[Title Page](#)[Abstract](#)[Introduction](#)[Conclusions](#)[References](#)[Tables](#)[Figures](#)[◀](#)[▶](#)[◀](#)[▶](#)[Back](#)[Close](#)[Full Screen / Esc](#)[Printer-friendly Version](#)[Interactive Discussion](#)